Numerical Simulation of Microfluidic Flow Using a Combination of Micro and Macro Computational Techniques: Scaling Issues

Tom Mautner
SPAWAR Systems Center San Diego, 92152, USA
mautner@spawar.navy.mil

ABSTRACT

Recent literature has demonstrated the possibilities of using configurable surfaces to enhance the flow of fluids in MEMS devices. Not only are surface properties important in fluid delivery, the inherent problems of diffusion only mixing due to laminar flow needs to be overcome to provide more efficient fluidics for bio-sensors. Work has begun to investigate the use of synthetic jets and manipulated surface properties to enhance low Reynolds number (Re<10) flow mixing. A Lattice Boltzmann Method (LBM) has been used to compute the flow field data, and the macro scale convection-diffusion equation was used to compute the passive scalar field. The main issue with this hybrid approach is proper scaling of the grid spacing and time increment between the micro and macro solution techniques. Results of the hybrid method as applied to Re<150 flows demonstrate the effects of scaling, and will be compared to an LBM multi-fluid method.

Keywords: Lattice Boltzmann, MEMS, microfluidics, scaling, mixing

1 INTRODUCTION

Recent literature has demonstrated the possibilities of using configurable surfaces to enhance the flow of fluids in MEMS devices. Not only are surface properties important in fluid delivery, the inherent problems of only diffusion mixing due to laminar flow needs to be overcome to provide more efficient fluidics for bio-sensors. Considering past macro scale CFD efforts and the use of reconfigurable surfaces [1-3], work has begun to investigate the use of synthetic jets and manipulated surface properties to enhance low Reynolds number (Re<10) flow mixing. While investigating the use of synthetic jets for fluid mixing in MEMS devices, it is necessary to compute both the fluid flow and concentration fields. The Lattice Boltzmann Method (LBM) has been used to compute the flow field data in these systems. In lieu of following the usual multi-fluid techniques found in the literature [5,6,8], a hybrid approach was used. The micro scale formulation of LBM was supplemented with a macro-scale, finite difference formulation of the convection-diffusion equation. While this seems easy enough, it became apparent that the main issue with this hybrid approach is proper scaling of the grid spacing and time increment between the micro and macro solution techniques. This work presents the results of the hybrid method as applied to Re<150 flows concentrating on the microfluidic regime of Re<10. The computation method uses algorithms which have been compared to results found in the literature. An LBM multi-fluid methods will provide additional comparisons.

2 METHOD

Lattice Boltzmann methods (LBM) have seen rapid expansion since the 1980's, and the LBM has proven to be a promising scheme for flows involving complex boundaries and interfacial dynamics [4]. Using a 9 component lattice BGK model, the Lattice Boltzmann equation is

$$\partial f_i / \partial t + e_i \bullet \nabla f_i = (f_i - f_i^{eq}) / \tau_v \qquad (1)$$

where e_i are the 9 BGK lattice velocities and f_i^{eq} is the equilibrium distribution. Equation (1) has been applied to the low Reynolds number, incompressible fluid flow in various two-dimensional geometries such as driven cavities, vortex shedding from rectangular cylinders, jets and channels.

The second part of the hybrid method computes the evolution of the concentration field, C. This is performed using the convection-diffusion equation

$$\partial C / \partial t + u \cdot (\nabla C) = (1/Pe) \nabla^2 u \qquad (2)$$

where the Peclet number is Pe=uL/D, D is the diffusion coefficient, L is a characteristic length and u is the velocity. The concentration equation is computed using an explicit finite-difference method with differencing based upon local velocity, (u,v), that is upwind/downwind differencing. In this paper, the concentration field is always considered to be a passive scalar.

To provide additional comparisons, the macro scale convection-diffusion equation was replaced by a second BGK type equation (g) to model the passive scalar field transport. This multi-fluid formulation follows the work of Flekkoy, et al [9,10]. In this case, the tracer field is computed using the same numerical method as that used for equation (1); however, it should be noted that the flow and tracer fields are independent. The concentration equation used is

$$\partial g_i / \partial t + e_i \bullet \nabla g_i = (g_i - g_i^{eq}) / \tau_D \quad (3)$$

The mass density, momentum density and concentration are determined using

$$\rho = \sum_i f_i \quad \rho u = \sum_i e_i f_i \quad C = \sum_i g_i \quad (4)$$

and τ_v and τ_D are the relaxation parameters based upon viscosity and diffusion respectively. The kinematic viscosity, v, and the diffusion coefficient, D, are related to the relaxation coefficients using the relationships

$$\nu = (2\tau_v - 1)/6 \text{ and } D = (2\tau_D - 1)/6 \quad (5)$$

Finally, the pressure is related to the density, ρ, by $p=c^2\rho$ where c=1/3 (9 point BGK model).

3 SCALING

The transport portion of the simulation is defined by a passive scalar equation in which the motion of the scalar is determined by the LBM computed velocity field. The use of a macro scale convection-diffusion equation in concert with the microscopic LBM requires examination of the scaling between the macro and micro length and time scales. The relevant fluid scales are the advective and momentum-diffusive time for the fluid and the mass diffusion time for the passive tracer. The Reynolds number, Re=UL/v, defines the momentum transport/momentum diffusivity while the Peclet number, Pe=UL/D, describes the mass transport/mass diffusivity relationship. What must be determined is the relationship between the micro and macro length and time scales for proper transport.

When considering LBM, it is necessary to distinguish between Boltzmann (LB) and Navier-Stokes (NS) scales [11]. Both have the same characteristic length scale L; however, the velocity scales differ. LBM uses a typical velocity of |c| while the NS formulation uses the velocity u which leads to the characteristic velocity of U. Using the length and velocity scales, the characteristic times for LBM and NS become $T_{LB}=L/|c|$ and $T_{NS}=L/U$. Since LBM describes a compressible gas and, when restricted to very low Mach numbers, approximates incompressible flow, one concludes that U/|c| is small. Setting $U/|c|=\varepsilon$ and using the scaled velocity u/U, one obtains $T_{LB}=\varepsilon T_{NS}$. In LBM lattice units, $\delta x=|c|\delta t$. The scaled time step $\delta t_{LB}=\delta t/T_{LB}$ and length $\Delta x=\delta x/L$ are used to obtain

$$\Delta t_{LB} = \delta t / T_{LB} = \delta x / L = \Delta x \quad (6)$$

The above relationship does not indicate the fact that it takes many LBM time steps to produce the macroscopic effects related to the flow velocity u where $\Delta t=\Delta x^2$. In non-dimensional variables and using the 9 point BGK model, the Reynolds number is related to the relaxation parameter and the LBM kinematic viscosity by

$$1/\mathrm{Re} = c^2 (2\tau_v - 1)/2 = (2\tau_v - 1)/6 = \nu_{LB} \quad (7)$$

The macroscopic time step is obtained from LBM scales using the fact that in LBM lattice units $\delta t=\delta x/|c|$ and $c=1/(3)^{1/2}$ (9 point BGK model).

Next, one requires a value for the diffusion coefficient. From the work of Flekkoy et al [9,10], one can extract D=0.00877 for $1/\tau_D$ =1.9. A Pe=10,000 was used in the convection-diffusion equation (2), and Pe lies within the acceptable range of Flekkoy et al's results. The relaxation parameter associated with the concentration equation (3) is obtained using equation (5).

4 SIMULATION RESULTS

The following are examples to demonstrate the effect of scaling on various flow configurations and Reynolds numbers. The first case considered involves application of both transport equations ((2) and (3)) in conjunction with the LBM flow field solution (Eqn. (1)). The remaining examples demonstrate the effect scaling in the hybrid method, via solution of equations (1) and (2).

4.1 Driven Cavity

The driven cavity problem was used as a benchmark in verifying the LBM solution technique in past work. For the work herein, the LBM velocity field was used by the transport equations to determine the passive tracer concentration as a function of time. The cavity grid was 160x160 with Δx=0.00625 for both Re=100 and Re=10. Also, Pe=10,000 and a lid velocity of $U_{LID}=0.1$ was used in all cases. Solutions for the stream function and vorticity contours yield results which are in excellent agreement with the literature [12].

Figure 1 compares the results for three values of Δt at Re=100 for both the hybrid and multi-fluid computation models. The scaling rules outlined above (section 3) determined Δt=0.0108; however, the hybrid method results with Δt=0.0054 (Fig. 1b) more closely agree with the LBM multi-fluid data (Fig. 1d). On the other hand, the Δt=0.0108 data shows a low concentration region in the same approximate region as the primary vortex determined by the velocity field.

The second set of driven cavity results are for Re=10 with three values of Δt. As in the Re=100 data, the LBM multi-fluid results agree more closely with the hybrid method using Δt=0.0054. Thus, one could conclude from

these results that the scaling rule Δt provides faster transport development than the multi-fluid method. However, the data does yield qualitatively useful results.

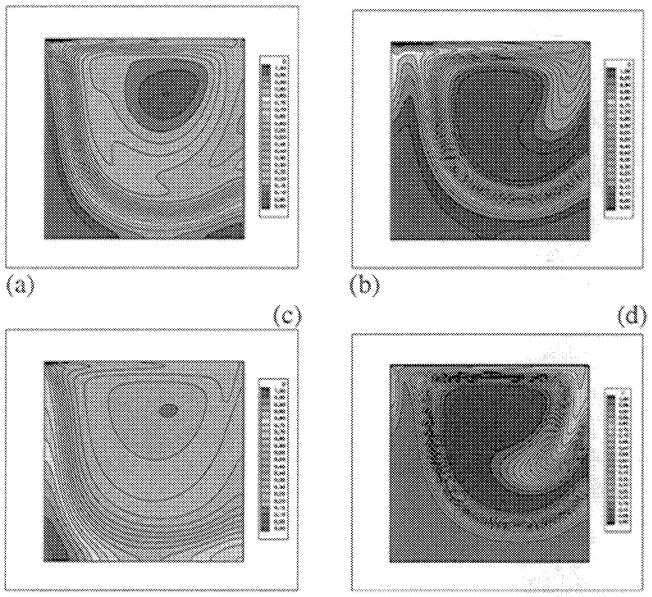

Figure 1. Concentration contours for driven cavity flow, Re=100, t=10,000. Eqn (2): a) Δt=0.0108; b) Δt=0.0054; and c) Δt=0.0216. Eqn. (3): d) D=0.00877.

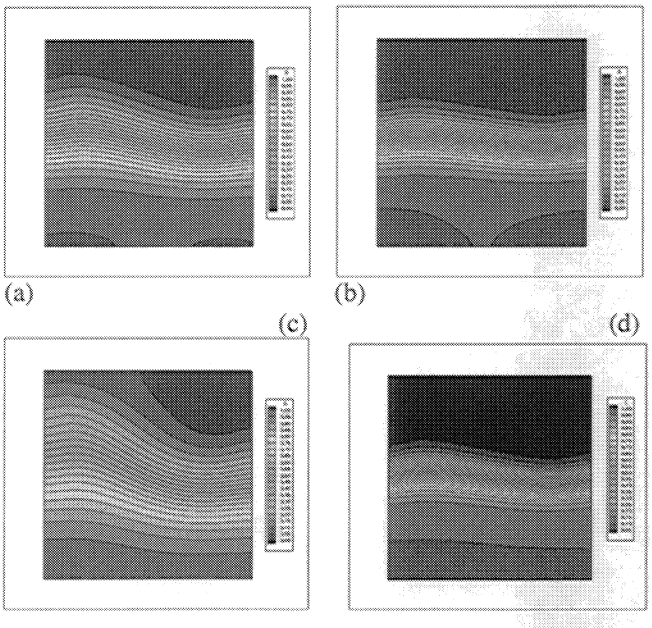

Figure 2. Concentration contours for driven cavity flow, Re=10, t=10,000. Eqn. (2): a) Δt=0.0108; b) Δt=0.0054; and Δt=0.0216. Eqn. (3): d) D=0.00877.

4.2 Vortex Shedding

In order to make an additional comparison with published data [13], the confined flow around a square cylinder was investigated. The two-dimensional channel had a blockage ratio of 1/5, a 501x101 grid with a uniform spacing of Δx=0.001 and a parabolic inlet velocity profile with a maximum value of u=0.1. A Re=150 was used to insure vortex shedding. As in the driven cavity case, three values of Δt were used with Δt=0.0173 obtained from the scaling law. As shown in figure 3, the usual von Kármán vortex street occurs. Examination of the computed results would indicate that the lower Δt=0.0086 may be more representative of the concentration field associated with the vortex shedding.

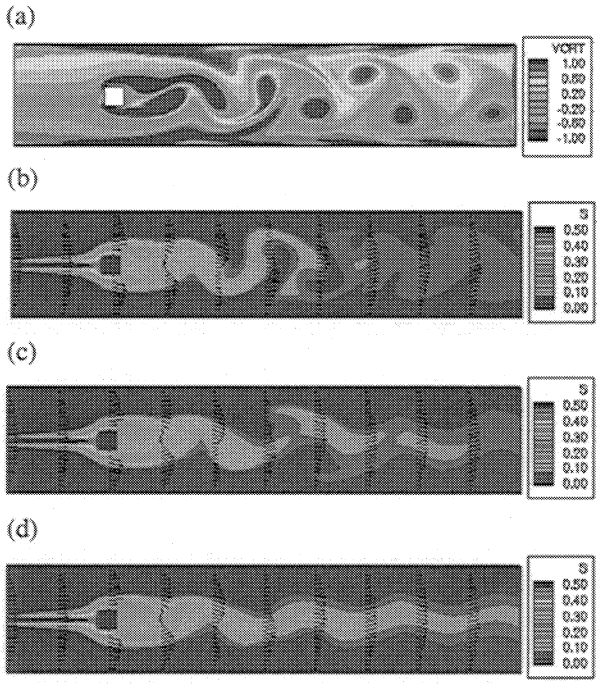

Figure 3. Vorticity and concentration contours (Eqn. (2)) for vortex shedding from a rectangular cylinder, Re=150, t=20,000. a) Vorticity. Tracer: b) Δt=0.0086; c) Δt=0.0173; d) Δt=0.0346.

4.3 Channel Flow with Synthetic Jets

Current work [15] involves the investigation of synthetic jets [14] to enhance fluid mixing in microfluidic devices. As in the examples above, a passive tracer was used to enhance visualization of the flow in the channel due to various Reynolds numbers and jet geometries. A sinusoidal, time dependent wall velocity drives the synthetic jet. The single jet results presented here had an overall grid size of 800x196 with the jet cavity having an aspect ratio of 1/5 while the jet inlet, to the channel, had an

aspect ratio of 1/1. The channel width was 160 grid points with a Δx=0.00625. A parabolic velocity profile formed the initial channel velocity field. For Re=1, the inlet maximum velocity was U_{IN}=0.00052 and the maximum jet cavity wall velocity was $5U_{IN}$. The details of the synthetic jet/channel study can be found in reference 15.

Two time steps were used to provide a comparison of time scale effects on the concentration distribution. In this case, experiments are required to provide verification of the simulated results; however, examination of the velocity and vorticity fields leads one to conclude that the smaller time step (Fig. 4a) would more accurately represent the tracer transport.

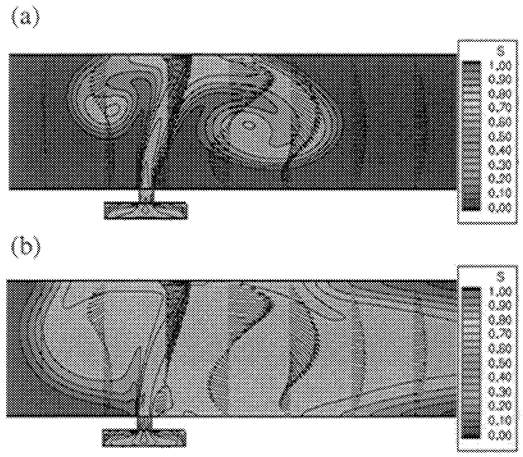

Figure 4. Concentration contours and velocity vectors for channel flow with a synthetic jet; Re=1, t=10,000: a) Δt=0.0054; b) Δt=0.0216.

5 CONCLUSIONS

The lattice Boltzmann method was used to compute the flow field for various test problems. The resulting velocity field was used to determine the transport properties of a passive scalar using two methods. Data computed using the convection-diffusion equation demonstrated results which were moderately dependent upon small changes in predicted scaling relationship for grid spacing and time step. Comparing results using a lattice Boltzmann multi-fluid method to compute the passive tracer field, one finds qualitative agreement in the concentration field distribution. Additional comparisons should be made using recent improvements in multiphase LBM methods.

REFERENCES

[1] A. Darhuber, J. Davis, W. Reisner, and S. Troian, "Thermocapillary Migration of Liquids on Patterened Surfaces: Design Concept for Microfluidic Delivery," MicroTas, 2001

[2] H. Stone, "Fluid Motion of Monomolecular Films in a Channel Flow Geometry," Phys. Fluids, 7, 1995

[3] C. Picioreanu, M. van Loosdrecht, and J. Heijen, "A Theoretical Study on the Effect of Surface Roughness on Mass Transport and Transformation in Biofilms," Biotech. & Bioeng., 68, 2000

[4] S. Succi, *The Lattice Boltzmann Equation for Fluid Dynamics and Beyond*, Clarendon Press, Oxford, 2001

[5] S. Succi, "Computational Multiphysics With the Lattice Boltxmann Equation," SIMU Newsletter, 3, 2001

[6] S. Hou, X. Shan, Q. Zou, G. Doolen and W. Soll, "Evaluation of Two Lattice Boltzmann Models for Multiphase Flows," J. Comp. Physics, 138, 1997

[7] B. Boghosian, P. Coveney, and A. Emerton,, "A Lattice-Gas Model of Microemulsions," Proc. R. Soc. London A, 452, 1996

[8] R. Zhang, X. He and S. Chen, "Interface and Surface Tension in Incompressible Lattice Boltzmann Multiphase Model," Comp. Physics Comm, 129, 2000

[9] E. Flekkoy, "Lattice Bhatnagar-Gross-Krook Models for Miscible Fluids," Phy. Rev. E, 47, 4247, 1993

[10] E. Flekkoy, U. Oxaal, J. Feder and T. Jossang, "Hydrodynamic Dispersion at Stagnation Points: Simulations and Experiments," Phy. Rev. E, 52, 4952, 1995

[11] M. Junk, "A Finite Difference Interpretation of the Lattice Boltzmann Method, Numer. Methods Part. Diff. Eqns., 17, 383, 2001

[12] S. Hou and Q. Zou, "Simulation of Cavity Flow by the Lattice Boltzmann Method," J. Comp. Phys., 118, 329, 1995

[13] M. Breuer, J. Bernsdorf, T. Zeiser and F. Durst, "Accurate Computations of the Laminar Flow Past a Square Cylinder Based on Two Different Methods: Lattice-Boltzmann and Finite Volume," Int. J. Heat Fluid Flow, 21, 2000

[14] R. Mittal and P. Rampunggoon, "Interaction of a Synthetic Jet with a flat Plate Boundary Layer," AIAA Paper 2001-2773, 2001

[15] T. Mautner, "Application of Synthetic Jets to Low Reynolds Number Biosensor Microfluidic Flows for Enhanced Mixing: A Numerical Study Using the Lattice Boltzmann Method," SPIE Smart Materials, Nano-, and Micro-Smart Systems, Paper 4937-23, Melbourne, AU, Dec., 2002